J. Phys. D: Appl. Phys. **43** (2010) 095101 (5pp) doi:10.1088/0022-3727/43/9/095101

Non-doped white organic light-emitting diodes based on aggregation-induced emission

Shuming Chen[1], Zujin Zhao[2], Ben Zhong Tang[2] and Hoi Sing Kwok[1,3]

[1] Center for Display Research, Department of Electronic and Computer Engineering, The Hong Kong University of Science and Technology, Clear Water Bay, Kowloon, Hong Kong
[2] Department of Chemistry, The Hong Kong University of Science and Technology, Clear Water Bay, Kowloon, Hong Kong

E-mail: eekwok@ust.hk

Received 16 October 2009, in final form 22 January 2010
Published 15 February 2010
Online at stacks.iop.org/JPhysD/43/095101

Abstract
Non-doped white organic light-emitting diodes (WOLEDs) based on newly synthesized bluish-green light-emitting material 1,3,6,8-tetrakis [4-(1,2,2-triphenylvinyl)phenyl]pyrene (TTPEPy) and red light-emitting material 4-(4-(1,2,2-triphenylvinyl)phenyl)-7-(5-(4-(1,2,2-triphenylvinyl)phenyl)thiophen-2-yl)benzo[c][1,2,5]thiadiazole (BTPETTD) have been demonstrated. A maximum efficiency of 7.4 cd A^{-1}, 4 lm W^{-1} and brightness of 18 000 cd m^{-2} have been achieved by employing 3 nm thick 4, 4′-bis [N-(1-naphthyl-1-)-N-phenyl-amino]-biphenyl (NPB) as an electron-blocking layer. The WOLEDs exhibit a high colour rendering index of 90 and moderate colour stability with 1931 Commision International de L'Eclairage coordinates changing from (0.41, 0.41) to (0.38, 0.40) over a wide range of driving voltages. Moreover, the non-doped WOLEDs enjoy a reduced efficiency roll-off due to their nature of aggregation-induced emission.

(Some figures in this article are in colour only in the electronic version)

1. Introduction

White organic light-emitting diodes (WOLEDs) have been of considerable interest in recent years due to their potential applications in display and lighting [1–11]. In general, various highly efficient fluorescent dyes such as DSA-ph, C545T and DCJTB, which emit different colours, are employed to construct the white colour [1–10]. Although the fluorescent quantum efficiency of most dyes approaches unity in their dilute solution, it decreases dramatically in the solid state due to strong intermolecular π–π stacking interaction, a notorious effect known as aggregation-caused quenching (ACQ) [12]. To alleviate the ACQ effect, usually the dyes are doped into host matrices to disperse the dye molecules so that a high efficiency can still be maintained even in the solid state [1–10, 15, 16]. Although doping is an effective method to address the problem of ACQ, it is sometimes problematic for the fabrication of WOLEDs, which in general require two or three fluorescent dyes to generate the white light emission. Moreover, a low doping concentration, ∼1% typically, is employed to mitigate the ACQ effect. It is extremely difficult to precisely control such low doping concentrations. Hence the reproducibility of doped-type fluorescent WOLEDs suffers, for the efficiency and chromaticity are doping concentration dependent. A variety of non-doped WOLEDs have been reported to overcome this drawback [2–8, 19]; however, most of the reports used an ultrathin layer of ∼1 Å of fluorescent dye such as C545T, DCJTB and rubrene as the emitting layer [2–8]. It is very difficult to accurately deposit such an ultrathin layer and thus this kind of non-doped WOLEDs does not simplify the fabrication process.

While the conventional dyes suffering from the ACQ effect may not be suitable for constructing highly efficient non-doped OLEDs, novel materials with non-planar propeller shape molecular structures exhibiting aggregation-induced emission (AIE) characteristics may be an ideal choice for non-doped OLEDs. In contrast to conventional dyes, these AIE materials are non-emissive in their dilute solution but emit intensely in the solid state due to restriction of intramolecular

[3] Author to whom any correspondence should be addressed.

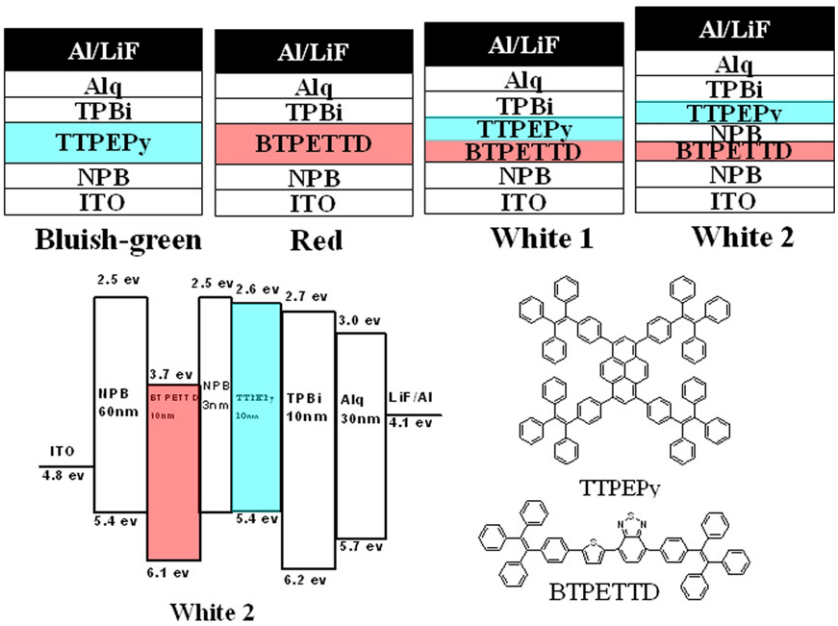

Figure 1. Schematic illustration of the device structures as well as the energy level and molecular structures.

rotation [12]. A series of highly efficient non-doped monochromatic OLEDs have been demonstrated based on AIE materials [13–16]. However, highly efficient non-doped WOLEDs based on AIE emitters have not yet been reported. In this work, we report non-doped WOLEDs based on newly synthesized bluish-green AIE material 1,3,6,8-tetrakis [4-(1,2,2-triphenylvinyl)phenyl]pyrene (TTPEPy) [15] and red AIE material 4-(4-(1,2,2-triphenylvinyl)phenyl)-7-(5-(4-(1,2,2-triphenylvinyl)phenyl)thiophen-2-yl)benzo[c] [1,2,5]thiadiazole (BTPETTD) [16]. We show that the efficiency, white colour purity, colour rendering index (CRI) and colour stability of the WOLEDs can be tuned by introducing different thicknesses of 4, 4′-bis [N-(1-naphthyl-1-)-N-phenyl-amino]-biphenyl (NPB) as an electron-blocking layer. The WOLEDs with 3 nm-thick NPB electron-blocking layer exhibit an efficiency of 7.4 cd A^{-1} and 4 lm W^{-1} with high CRI of 90, while the WOLEDs with a 4 nm thick NPB electron-blocking layer show an impressive colour stability with CIE coordinates changing from (0.34, 0.42) to (0.34, 0.40) over a wide range of driving voltages. Moreover, the non-doped WOLEDs enjoy a reduced efficiency roll-off due to their nature of AIE.

2. Experiment

The TTPEPy and BTPETTD were synthesized according to [15, 16]. Other organic materials were purchased from Lumtec without further purification. The devices were fabricated on 80 nm thick ITO coated glass with a sheet resistance of 25 Ω/□. The structures of the fabricated devices as well as the energy level and molecular structures of the emitters are shown in figure 1. In these devices, a 20 nm thick TTPEPy, a 20 nm thick BTPETTD and a 10 nm thick TTPEPy combined with 10 nm thick BTPETTD were employed as the light-emitting layer for the bluish-green, red and white OLEDs, respectively. For the white 2 OLEDs, a 3 nm thick NPB layer was inserted between the TTPEPy and BTPETTD serving as the electron-blocking layer. A 60 nm thick NPB, a 10 nm thick 2, 2′, 2″-(1, 3, 5-benzinetriyl) tris(1-phenyl-1-H-benzimidazole) (TPBi) and a 30 nm thick tris (8-hydroxyquinoline) aluminium (Alq_3) were used as hole-transporting, hole-blocking and electron-transporting layers, respectively. All organic layers in the devices were thermally evaporated in sequence in a multi-source vacuum chamber at a base pressure of around 5×10^{-7} Torr. The samples were then transferred to the metal chamber without breaking vacuum for cathode deposition which was composed of 1 nm thick LiF capped with 100 nm thick Al. The light-emitting area was 4 mm^2 defined by the overlap of cathode and anode. The current density–voltage characteristics of the devices were measured by the HP4145B semiconductor parameter analyser. The forward direction photons emitted from the devices were detected by placing a calibrated UDT PIN-25D silicon photodiode very close onto the top of the devices. The luminance and external quantum efficiency of the devices were inferred from the photocurrent of the photodiode. The electroluminescent (EL) spectra were obtained with the PR650 spectrophotometer. All measurements were carried out under ambient conditions without device encapsulation.

3. Results and discussion

Figure 2(*a*) compares the typical voltage–luminance–current density characteristics of the devices. It is obvious that the bluish-green devices exhibit a substantially smaller current density compared with the red devices, which may be mainly due to the lower lowest unoccupied molecular orbital (LUMO) level (figure 1) of TTPEPy compared with that of BTPETTD, resulting in larger electron injection barrier in the bluish-green devices compared with that in the red devices. The current density of the white devices lies

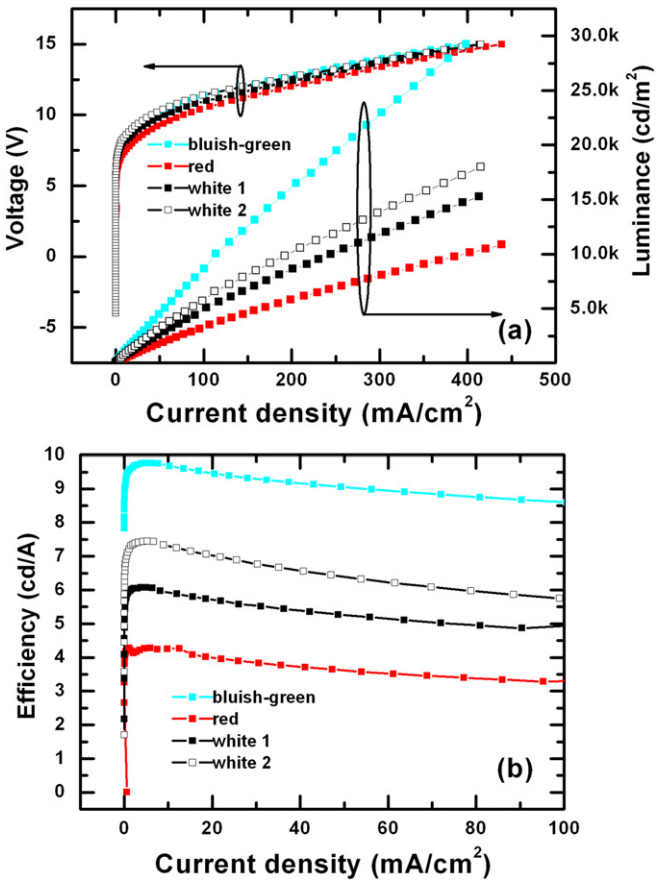

Figure 2. (*a*) Voltage–luminance–current density and (*b*) EL efficiency–current density characteristics of the devices.

between that of the bluish-green and the red devices; white 2 devices with 3 nm thick NPB electron-blocking layer exhibit smaller current density compared with white 1 devices, which is expected since the introduction of a NPB layer increases the total thickness of white 2 devices, and more importantly, blocks some of the electrons transporting from TTPEPy to BTPETTD for the electron mobility of NPB is extremely low [9–11]. The luminance increases rapidly with the increase in current density for all devices. At a current density of 100 mA cm^{-2}, the bluish-green devices show a luminance of 8660 cd m^{-2}, significantly higher than 5700 cd m^{-2}, 5103 cd m^{-2} and 3600 cd m^{-2} for the white 2, white 1 and red devices, respectively.

As shown in figure 2(*b*), the peak current efficiency of the bluish-green and red devices is around 9.8 cd A^{-1} and 4.2 cd A^{-1}, respectively, which are among the best value for the fluorescent bluish-green and red OLEDs previously reported [14, 17, 18]. The efficiency of the white devices lies between that of the bluish-green and red devices. By introducing a 3 nm thick NPB electron-blocking layer, white 2 devices exhibit a peak current efficiency of 7.4 cd A^{-1}, substantially higher than 6 cd A^{-1} for the white 1 devices. Such efficiency improvement is due to more even excitons distribution in white 2 devices. Without the NPB electron-blocking layer, most excitons recombine in the BTPETTD layer due to its higher LUMO level compared with TTPEPy (figure 1), resulting in lower efficiency due to the lower light-emitting efficiency of BTPETTD. With 3 nm thick electron-blocking layer, more electrons are confined in the TTPEPy layer due to the poor electron-transporting property of NPB, leading to an even excitons distribution and hence higher efficiency in white 2 devices. In contrast to most of the doped-type fluorescent OLEDs, which suffer from tremendous efficiency roll-off at high doping concentration due to the notorious ACQ effect, all devices studied here show an impressive stability of efficiency due to their AIE nature. For instance, even at a high brightness of 5000 cd m^{-2}, the efficiency only slightly rolls off to 9 cd A^{-1}, 6 cd A^{-1}, 5 cd A^{-1} and 3 cd A^{-1} for the bluish-green, white 2, white 1 and red devices, respectively.

Figure 3(*a*) shows the spectra of the white 1 devices under different driving voltages as well as the spectra of the bluish-green devices and the red devices. Multiple-emission peaks centred at 524 nm, 492 nm and 472 nm were observed for the bluish-green devices. The peak of 492 nm is originated from TTPEPy [15], while other peaks are attributed to impurities. It should be noted that we only purified TTPEPy by boiling it in THF followed by filtrating, which is impossible to eliminate all of the metal catalysts. With cleaner TTPEPy, the efficiency would be further improved. Indeed, we have achieved a current efficiency of 12 cd A^{-1} and an external quantum efficiency of 5% in bluish-green OLEDs using cleaner TTPEPy [15]. Inspite of this disadvantage, efficient and bright bluish-green, red and WOLEDs were obtained (figure 3(*e*)). As shown in figure 3(*a*), the bluish-green emission decreases as voltages increase, mainly because more excitons recombine in the BTPETTD layer with increased voltages, resulting in CIE coordinates and colour correlate temperature (CCT) changing from (0.42, 0.39), 3268 K at 6 V to (0.45, 0.39), 2672 K at 14 V. In order to obtain a purer white colour, the bluish-green emission should be enhanced; thus it is necessary to introduce the NPB electron-blocking layer. To investigate the dependence of WOLEDs spectra on the thickness of the NPB electron-blocking layer, three WOLEDs with NPB thickness of 2, 3 and 4 nm were fabricated. Figures 3(*b*)–(*d*) show the spectra of the WOLEDs with different thicknesses of NPB electron-blocking layer. It is obvious that the bluish-green emission is boosted significantly by introducing a NPB electron-blocking layer, clearly demonstrating that the NPB can block the electrons effectively. Interestingly, in contrast to the white 1 devices with bluish-green emission decreasing monotonically as driving voltages increase, the bluish-green emission decreases when the voltages change from 6 to 8 V and then gradually increases when the voltages change from 10 to 14 V for all devices employing a NPB electron-blocking layer. Such phenomena can be explained by taking into account the energy level of BTPETTD. As shown in figure 1, the highest occupied molecular orbital (HOMO) level of BTPETTD is 6.1 eV, leading to a high hole-injection barrier at the BTPETTD/NPB hole-transporting layer interface. At low driving voltages (<8 V), most holes may not gain sufficient energy to overcome such a high barrier; thus most of them accumulate at BTPETTD/NPB hole-transporting layer interface. As the voltages keep increasing, more and more electrons are injected from TTPEPy to BTPETTD, resulting in a decreased bluish-green emission. However, when the

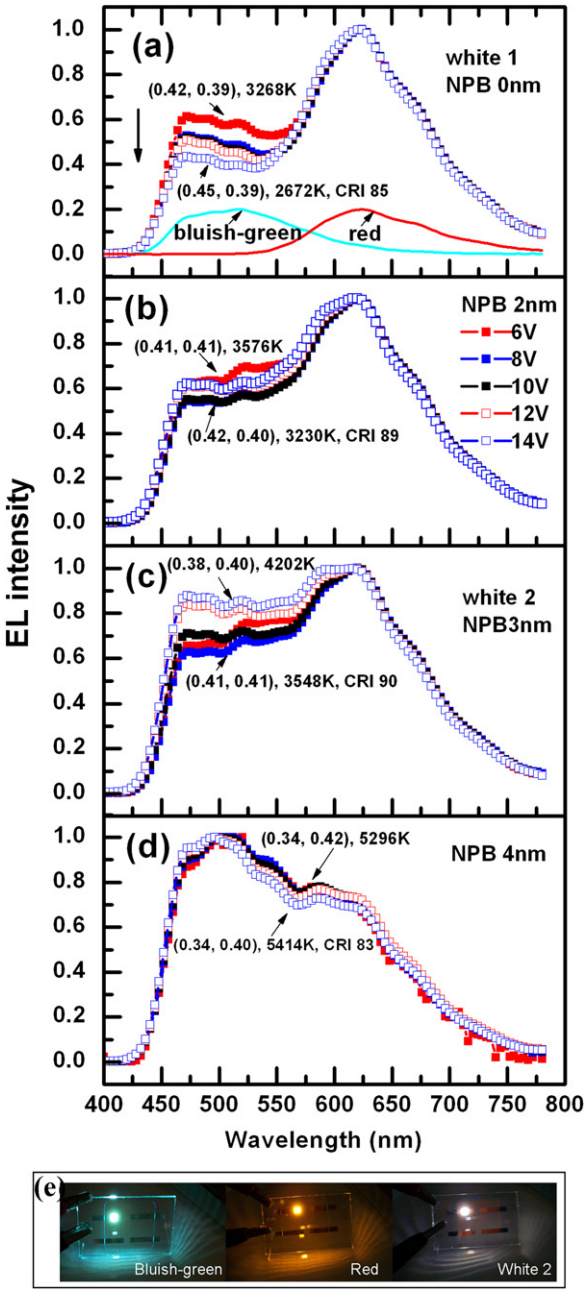

Figure 3. (*a*) EL spectra of the bluish-green, red and white 1 devices, (*b*)–(*d*) EL spectra of white devices with 2, 3 and 4 nm NPB layer, respectively, under different driving voltages and (*e*) photos of bluish-green, red and white 2 devices.

driving voltages are larger than 8 V, the holes may tunnel through the high barrier and inject from NPB to BTPETTD. With the help of the thin NPB electron-blocking layer, the holes can further diffuse to TTPEPy smoothly, hence leading to a gradually enhanced bluish-green emission with increased driving voltages, as shown in figures 3(*b*)–(*d*). Such enhanced bluish-green emission further shifts the CIE coordinates and CCT to the equivalent white energy point. Take the white devices with the 3 nm thick NPB electron-blocking layer for example, the CIE coordinates and CCT change from (0.41, 0.41), 3548 K at 8 V to (0.38, 0.40), 4202 K at 14 V, while the white devices with the 4 nm thick NPB electron-blocking layer

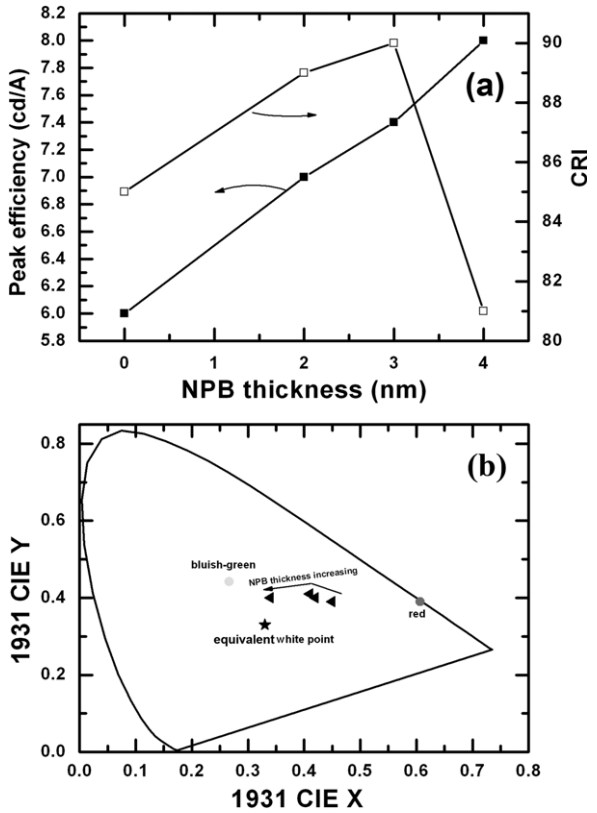

Figure 4. (*a*) The dependence of peak efficiency and CRI on NPB thickness, (*b*) CIE coordinates of the white devices with different NPB thicknesses.

show an impressive colour stability with the CIE coordinates and CCT change from (0.34, 0.42), 5296 K at 8 V to (0.34, 0.40), 5414 K at 14 V.

It is also noted that the bluish-green emission is enhanced gradually with increased thickness of the NPB electron-blocking layer, as shown in figures 3(*b*)–(*d*). Thus the thickness of the NPB electron-blocking layer plays a crucial role in adjusting the efficiency, CIE coordinates, CRI and colour stability of the white devices. Figure 4 shows the dependence of peak efficiency, CRI at 1000 cd m^{-2}, and CIE coordinates at 1000 cd m^{-2} on the thickness of the NPB electron-blocking layer. The efficiency increases monotonically as NPB thickness increases, which is mainly due to more excitons confined in the highly efficient bluish-green emitter by blocking the electron diffusion to the relatively low efficiency red emitter. Furthermore, the CIE coordinates are shifted close to (0.33, 0.33) by increasing the thickness of the NPB, changing from (0.45, 0.39) for the white device without the NPB electron-blocking layer to (0.34, 0.40) for the white devices with the 4 nm thick NPB electron-blocking layer, as shown in figure 4(*b*). Although a higher efficiency and purer white colour would be obtained by further increasing the thickness of NPB, the CRI rolls off with increased NPB thickness due to the reduction of red emission (figure 4(*a*)). For example, the CRI at 1000 cd m^{-2} increases from 85, 89 to 90 and then rolls off significantly to 81 as the NPB thickness increases from 0, 2, 3 to 4 nm. Thus, there is a trade-off between efficiency, white colour purity and CRI. It should

Table 1. Performance of the devices.

Device	V (V) at 1 K cd m^{-2}	L (cd m^{-2}) at 15 V	$\eta_{L_{max}}$ (cd A^{-1})	$\eta_{P_{max}}$ (lm W^{-1})	CIE (x, y) at 6 V	CIE (x, y) at 14 V	CRI at 14 V
Bluish-green	8.2	30 000	9.8	6.0	(0.26, 0.44)	(0.26, 0.44)	—
Red	8	11 000	4.2	2.7	(0.61, 0.39)	(0.61, 0.39)	—
White 1	8.2	15 000	6.0	3.2	(0.42, 0.39)	(0.45, 0.39)	85
White 2	8.3	18 000	7.4	4.0	(0.40, 0.42)	(0.45, 0.40)	90

be noted that, for lighting applications, a high CRI is more desirable than a pure white colour. Hence, to make a balance between efficiency, white colour purity and CRI, the NPB electron-blocking layer with a thickness of 3 nm is optimal for the white devices studied here. The key characteristics of the devices are listed in table 1.

4. Conclusion

In conclusion, non-doped WOLEDs based on AIE emitters have been demonstrated for the first time. Due to their AIE nature, the devices exhibit reduced efficiency roll-off. The efficiency, white colour purity, CRI and colour stability can be tuned by changing the thickness of the NPB electron-blocking layer. The WOLEDs with the 3 nm thick NPB electron-blocking layer exhibit an efficiency of 7.4 cd A^{-1} and 4 lm W^{-1} with a high CRI of 90, while the WOLEDs with a 4 nm thick NPB electron-blocking layer show an impressive colour stability with CIE coordinates changing from (0.34, 0.42) to (0.34, 0.40) over a wide range of driving voltages. Compared with conventional doped-type WOLEDs [1] or other non-doped WOLEDs [2–8] having performance sensitive to doping concentrations or ultrathin layer thickness, thus requiring stringent fabrication conditions, the non-doped WOLEDs studied here may be more suitable for mass production due to their simplicity of fabrication.

Acknowledgment

This work was supported by the Hong Kong Government Research Grants Council under Grant Number 614807.

References

[1] Zhang Z, Wang Q, Dai Y, Liu Y, Wang L and Ma D 2009 *Org. Electron.* **10** 491
[2] Tsuji T, Naka S, Okada H and Onnagawa H 2002 *Appl. Phys. Lett.* **81** 3329
[3] Yang H, Zhao Y, Xie W, Shi Y, Hu W, Meng Y, Hou J and Liu S 2006 *Semicond. Sci. Technol.* **21** 1447
[4] Yang H, Shi Y, Zhao Y and Liu S 2008 *Solid-State Electron.* **52** 657
[5] Yang H, Zhao Y, Hou J and Liu S 2006 *Displays* **27** 183
[6] Xie W, Wu Z, Liu S and Lee S T 2003 *J. Phys. D: Appl. Phys.* **36** 2331
[7] Xie W, Wu Z and Liu S 2004 *Opt. Quantum Electron.* **36** 635
[8] Li L, Yu J, Tang X, Wang T, Li W and Jiang Y 2008 *J. Lumin.* **128** 1783
[9] Wang Q, Ding J, Cheng Y, Wang L and Ma D 2009 *J. Phys. D: Appl. Phys.* **42** 065106
[10] Guo F, Ma D, Wang L, Jing X and Wang F 2005 *Semicond. Sci. Technol.* **20** 310
[11] Ho C L, Wong W Y, Wang Q, Ma D, Wang L and Lin Z 2008 *Adv. Funct. Mater.* **18** 928
[12] Hong Y, Lama W Y and Tang B Z 2009 *Chem. Commun.* 4332
[13] Chen H Y, Lam W Y, Luo J D, Tang B Z, Wong M and Kwok H S 2002 *Appl. Phys. Lett.* **81** 574
[14] Chen H, Chen J, Qiu C, Tang B Z, Wong M and Kwok H S 2004 *IEEE J. Sel. Top. Quantum Electron.* **10** 10
[15] Zhao Z, Chen S, Lam W Y, Lu P, Zhong Y, Wong K S, Kwok H S and Tang B Z 2010 *Chem. Commun.* at press, doi:10.1039/b921451h
[16] Zhao Z, Lam W Y and Tang B Z 2010 *Curr. Org. Chem.* at press
[17] Hwanga D H, Leea J D, Chob H J, Chob N S, Leeb S K, Parkc M J, Shimb H K and Leed C 2008 *Synth. Met.* **158** 802
[18] Haq K U, Liu S P, Khan M A, Jiang X Y, Zhang Z L and Zhu W Q 2008 *Semicond. Sci. Technol.* **23** 035024
[19] Yeh S J, Chen H Y, Wu M F, Chan L H, Chiang C L, Yeh H C, Chen C T and Lee J H 2006 *Org. Electron.* **7** 137